Sub-diffraction negative and positive index modes in mid-infrared waveguides

Anthony J. Hoffman[1,*], Viktor A. Podolskiy[2], Deborah L. Sivco[3], and Claire Gmachl[1]

[1]*Department of Electrical Engineering, Princeton University, Princeton, NJ, 08544, USA*
[2]*Physics Department, Oregon State University, Corvallis, OR, 97331, USA*
[3]*Alcatel-Lucent, Murray Hill, NJ 07974*
[*]*Corresponding author: ajhoffma@princeton.edu*

Abstract: We characterize a strongly anisotropic waveguide consisting of alternating 80 nm layers of n^+-InGaAs and i-AlInAs on InP substrate. A strong increase in the transverse magnetic (TM) reflection at λ = 8.4 μm corresponds to a characteristic low-order mode cutoff for the left-handed waveguide. The subsequent decrease of TM reflection at λ = 11.5 μm represents the onset of right-handed no-cutoff light guiding. Good qualitative agreement is found when the experimental results are compared to finite element and transfer-matrix frequency domain simulations.

OCIS codes: (160.1190) Anisotropic optical materials; (160.3918) Metamaterials; (160.6000) Semiconductor materials; (230.7370) Waveguides

References and links

1. R. A. Shelby, D. R. Smith, and S. Schultz, "Experimental Verification of a Negative Index of Refraction," Science **292**, 77 – 79 (2001).
2. V. M. Shalaev, "Optical negative-index metamaterials," Nat. Photonics **1**, 41 – 48 (2007).
3. D. R. Smith and D. Schurig, "Electromagnetic Wave Propagation in Media with Indefinite Permittivity and Permeability Tensors," Phys. Rev. Lett. **90**, 077405 (2003).
4. D. R. Smith, S. Schurig, J. J. Mock, P. Kolinko, and P. Rye, "Partial focusing of radiation by a slab of indefinite media," Appl. Phys. Lett. **84**, 2244 – 2246 (2004).
5. A. J. Hoffman, L. Alekseyev, S. S. Howard, D. Wasserman, V. A. Podolskiy, E. E. Narimanov, D. L. Sivco, and C. Gmachl, "Negative refraction in semiconductor metamaterials," Nat. Mater. **6**, 946 – 950 (2007).
6. J. Yao, Z. Liu, Y. Liu, C. Sun, G. Bartal, A. M. Stacy, and X. Zhang, "Optical Negative Refraction in Bulk Metamaterials of Nanowires," Science **321**, 930 (2008).
7. J. Elser and V. A. Podolskiy, "Scattering free plasmonic optics with anisotropic metamaterials," Phys. Rev. Lett. **100**, 066402 (2008).
8. J. Elser, A. A. Govyadinov, I. Avrustky, I. Salakhutdinov, V. A. Podolskiy, "Plasmonic nanolayer composites: coupled plasmon polaritons, effective-medium response, and subdiffraction light manipulation," J. Nanomaterials, **2007**, 79469 (2007).
9. A. A. Govyadinov and V. A. Podolskiy, "Subdiffraction light propagation in fibers with anisotropic dielectric cores," Phys. Rev. B. **75**, 155108 (2006).
10. Z. Jacob, L. V. Alekseyev, and E. E. Narimanov, "Optical Hyperlens: Far-field imaging beyond the diffraction limit," Opt. Express **14**, 8247 – 8256 (2006).
11. V. A. Podolskiy and E. E. Narimanov, "Strongly anisotropic waveguide as a nonmagnetic left-handed system," Phys. Rev. B **71**, 201101 (2005).
12. V. G. Veselago, "Electrodynamics of substances with simultaneously negative values of sigma and mu," Sov. Phys. Usp. **10**, 509 (1968).
13. J. B. Pendry, "Negative refraction makes a perfect lens," Phys. Rev. Lett. **85**, 3966 – 3969 (2000).
14. D. R. Smith and J. B. Pendry, "Homogenization of metamaterials by field averaging," J. Opt. Soc. Am. B **23**, 391 (2006).
15. J. Elser, V. A. Podolskiy, I. Salakhutdinov, and I. Avrutsky, "Nonlocal effects in effective-medium response of nanolayered metamaterials," Appl. Phys. Lett **90**, 191109 (2007).
16. www.comsol.com
17. V. V. Shevchenko, *Continuous transitions in open waveguides* (Golem Press, Boulder, 1971).
18. J. Elser, R. Wangber, V. A. Podolskiy, and E. E. Narimanov, "Nanowire metamaterials with extreme optical anisotropy," Appl. Phys. Lett. **89**, 261102 (2006).

#100752 - $15.00 USD Received 29 Aug 2008; revised 25 Sep 2008; accepted 25 Sep 2008; published 29 Sep 2008

1. Introduction

The first demonstration of negative refraction spurred a large interest in artificially structured materials, called metamaterials, with rare or previously non-existent optical properties [1-6]. Anisotropic metamaterials with indefinite permittivity and permeability tensors, one class of these materials, have shown good potential for photonic applications because of their unique interaction with light [3]. We previously demonstrated that light incident on such a strongly anisotropic metamaterial refracts negatively [5]. Additionally, it has been shown theoretically that such materials are capable of subwavelength imaging, subwavelength confinement, and scattering-free plasmonic optics [8-10]. Here, we study a strongly anisotropic material in a waveguide configuration. As was previously proposed, such a waveguide behaves as a left-handed system for the transverse magnetic (TM) polarization [11]. It was also shown that at different wavelengths, the same structure may support a set of highly confined right-handed modes [8, 9]. Using reflection measurements, we demonstrate the characteristic low-order-mode cutoff for the left-handed waveguide and the absence of a cut-off for right-handed highly confined modes.

The propagation of modes inside a waveguide is described by the dispersion relation. For extraordinary and ordinary modes in a waveguide with uniaxial anisotropy, the dispersion relation is given by: $k_z^2 + k_y^2 = \varepsilon^{(e|o)} v^{(e|o)} k^2$ where $\varepsilon^{(e)} = \varepsilon_\perp$, $\varepsilon^{(o)} = \varepsilon_{||}$, $v^{(e|o)} = 1-\chi^{(e|o)2}/(\varepsilon_{||} k^2)$ [11]. Here, k_y, k_z, and k are the y-component, z-component, and magnitude of the wave vector respectively; $\varepsilon_{||} = \varepsilon_{yy} = \varepsilon_{zz}$ and $\varepsilon_\perp = \varepsilon_{xx}$ are the components of the permittivity tensor as shown in Fig. 1; χ is a modal parameter of the waveguide that is proportional to mode order and is inversely proportional to the mode confinement scale; it can be solved analytically for simple geometries or numerically for more complicated structures; and (e) or (o) designate the extraordinary and ordinary waves respectively. The modal index, n, is given by $n = (\varepsilon v)^{1/2}$ [11]. When v and ε have different signs, the waves decay exponentially. Modes with positive v and ε have positive n and modes with negative v and ε have negative n. For modes with negative n, the phase velocity is in a direction opposite to the wave propagation and the waveguide behaves as a complete two-dimensional analog of three-dimensional negative index materials [12, 13].

The metamaterial used in this study is composed of alternating layers of semiconductor material with positive and negative permittivities. The layers are subwavelength and act as a metamaterial with optical properties that can be calculated using the effective medium approximation [14, 15]. In this study $\varepsilon_\perp$ is negative for a large bandwidth in the mid-infrared and v can be negative if χ is sufficiently large. Since larger χ corresponds to higher order modes, this condition results in a cutoff for low order modes. In our experiment, we demonstrate this cutoff by showing an increase in reflection at wavelengths where the sample transitions into the region of strong anisotropy where $\varepsilon_\perp < 0$ and $\varepsilon_{||} > 0$.

2. Material and experimental setup

The material used for this study was grown by molecular beam epitaxy (MBE) on semi-insulating InP substrate. The structure consisted of alternating 80 nm thick layers of $In_{0.53}Ga_{0.47}As$ and $Al_{0.48}In_{0.52}As$. In total, the epitaxial layer was 20 μm thick. The InGaAs layers were highly Si doped, measured as $n_d = 7.9 \times 10^{18}$ cm^{-3}, to provide a plasma resonance of free electrons at mid-infrared wavelengths. For the measurements, the epitaxial layer serves as an anisotropic waveguide with air and InP cladding. To determine the optical anisotropy, the sample was first characterized using reflection and transmission measurements as described in a previous publication [5]. Figure 1 shows the calculated values of $\varepsilon_\perp$ and $\varepsilon_{||}$ versus wavelength obtained using the effective medium approximation for the particular doping level, n_d, measured during characterization.

#100752 - $15.00 USD Received 29 Aug 2008; revised 25 Sep 2008; accepted 25 Sep 2008; published 29 Sep 2008

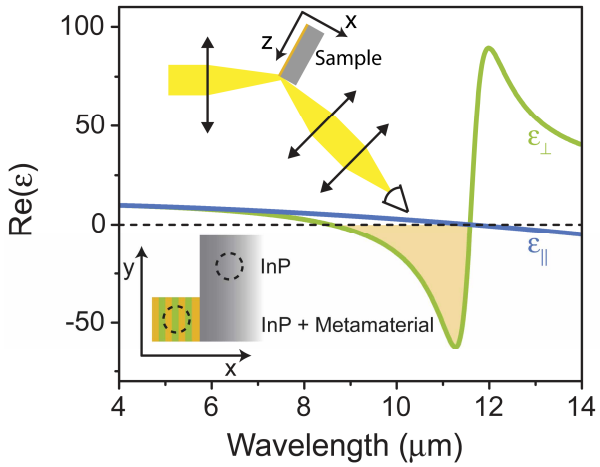

Fig. 1. Calculated values of $\varepsilon_{\|}$ and $\varepsilon_{\perp}$ versus wavelength using the effective medium approximation for a metamaterial with n_d = 7.9 x 10^{18} cm^{-3}. The shaded yellow region marks the spectral region where modes of sufficiently high order have negative n. The top left inset shows a schematic of the experimental setup and the bottom left inset shows a schematic of the sample used in the experiment and the definition of the coordinate system. The dashed circles show the location of the center of the incident beam for the different measurements.

The sample was prepared by cleaving a 1.0 x 2.0 cm^2 piece of the wafer. For the top 1.0 x 1.0 cm^2 portion of the sample, the epitaxial layer was removed using a $HBr:HNO_3:H_2O$ (1:1:10) etch. The sample was then cleaved down the center to yield two 0.5 x 2.0 cm^2 pieces with smooth facets. The bottom inset of Fig. 1 depicts the facet of a sample used in the experiments.

Reflection measurements were performed on both parts of the samples (without and with the metamaterial). Light from a Fourier Transform infrared (FTIR) spectrometer was linearly polarized, focused to a ~200 μm diameter spot using a 6 inch focal length ZnSe lens, and collected on a cooled HgCdTe (MCT) detector. The top portion of the sample (InP only) was located at the focal point of the focusing lens, as shown in the top inset of Fig. 1, the measured reflected light was maximized by translating the sample perpendicular to the incident beam, and spectra for the TM and transverse electric (TE) polarizations were collected. The sample was then translated vertically so that the spectra for the metamaterial and substrate could be collected for the same angle. The sample was first positioned such that the collected light was a maximum for the TM polarization. It was then shifted such that the power for the TM polarization was half the value previously recorded, thus locating the point of peak intensity closer to the metamaterial. This measurement was repeated for several angles; each spectrum was averaged over 400 scans.

3. Results

3.1 Experimental results

To remove the effects of reflection from the InP substrate, the data was analyzed as the ratio of the reflection measured for the part of the sample with the epitaxial layer, $R_{InP+meta}$, to the part with the epitaxial layer removed, R_{InP}. The reflection data for several angles are plotted in Fig. 2(a). The curves are offset because a comparison of the absolute value of the ratio is difficult due to the sensitivity of the location of the sample relative to the center of the incident beam. The relative changes in reflection versus wavelength for a single angle are preserved however.

#100752 - $15.00 USD Received 29 Aug 2008; revised 25 Sep 2008; accepted 25 Sep 2008; published 29 Sep 2008

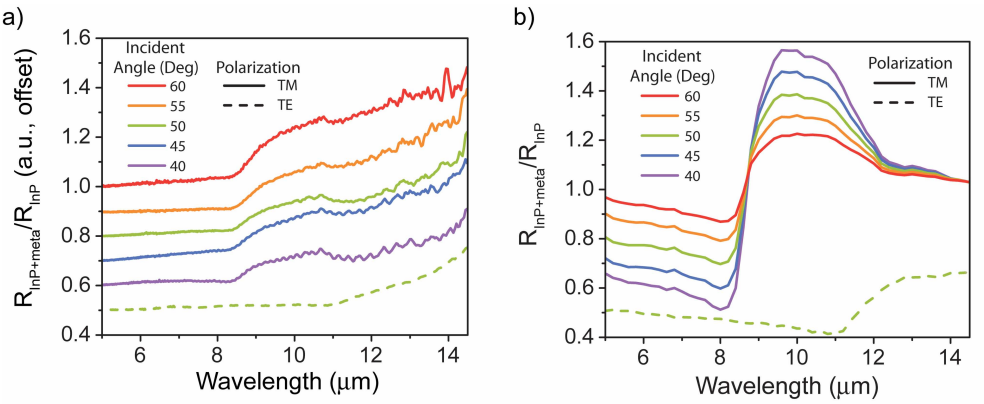

Fig. 2. (a). Measured ratio of the reflectance from the InP and metamaterial, $R_{InP+meta}$, to the reflectance of the InP, R_{InP}, for several incident angles. The solid lines are for the TM polarization and the dashed line is for the TE polarization with an incident angle of 50º. The data are linearly spaced. (b). Finite element frequency domain calculations of the ratio of the reflectance from the InP and metamaterial, $R_{InP+meta}$, to the reflectance of the InP, R_{InP}, for several incident angles. The solid lines are for the TM polarization and the dashed line is for the TE polarization with an incident angle of 50º.

As seen in the data, at approximately λ = 8.4 μm, there is a sharp increase in the TM reflection ratio. This increase in the ratio is due to a sharp increase in the reflection off the metamaterial layer which is due to the sudden change in its permittivity tensor. At this wavelength, $\varepsilon_{\perp} < 0$ and the lower order modes cannot propagate inside of the waveguide and are thus expelled [8, 9].

Around λ = 11 μm there is a sharp increase in the TE reflection and a small drop in the TM reflection, corresponding to the change in the sign of both $\varepsilon_{\perp}$ and $\varepsilon_{\parallel}$. As result of this change in the anisotropy of the metamaterial, the waveguide becomes opaque to all TE modes, increasing the reflection. The simultaneous drop in the TM reflection around this wavelength signifies the onset of cutoff-less propagation of right-handed modes; however, the large impedance mismatch between the metamaterial waveguide and vacuum at this wavelength significantly reduces the observed effect.

3.2 Numerical calculations

To gain insight into the observed phenomena, we performed two sets of numerical simulations. In the first set of calculations, the experiment was simulated using a commercial finite element (FE) frequency domain program [16]. In these calculations, the epitaxial layer was approximated as a uniaxial, anisotropic effective medium with a dispersion relation as described in a previous publication [5] and the InP substrate had an isotropic index of refraction, n = 3.1. Reflection as a function of wavelength, incident angle and beam width was studied for the system. Figure 2(b) shows the results of the calculations for a 30 μm diameter beam.

As with the experimental measurements, at λ = 8.4 μm there is a large increase in the TM reflection ratio. Also at $\lambda \sim$ 11 μm there is a dip in the TM ratio and an increase in the TE ratio. The magnitude of variation in reflectivity strongly depends on the beam diameter with wider beams yielding lower contrast. This effect is responsible for the quantitative discrepancy between numerical simulations and experimental results.

Further analysis of the numerical simulations demonstrates that the origin of variation in reflectivity is two-fold. First, a quantitatively weak contribution comes from negative refraction of the part of the beam that is incident on the top of the structure and is refracted towards the front interface. The main contribution comes from the unique negative-index waveguide's cutoff behavior. The mismatch between the field profiles of the incident beam and the waveguide modes results in the excitation of the whole spectrum of modes. Incident

#100752 - $15.00 USD Received 29 Aug 2008; revised 25 Sep 2008; accepted 25 Sep 2008; published 29 Sep 2008

light preferentially couples into lower-order waveguide modes; however, since these modes do not propagate in the negative index regime, the radiation is mostly reflected from the structure. The quantitatively small (although non-zero) propagation in the waveguide field is limited to higher order modes. At λ = 11.5 μm the signs of the components of the effective permittivity flip, and the waveguide begins transmitting all its TM modes, regardless of the mode number. At the same wavelength all TE modes cut off. This regime, known as positive-index photonic funnel [8, 9], is signified by a decrease of the reflectivity of TM modes.

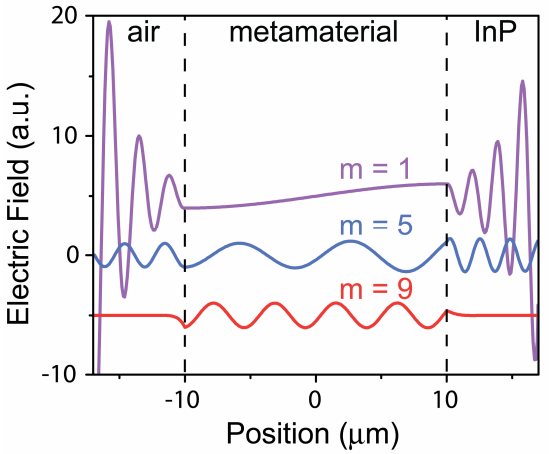

Fig. 3. Select mode profiles calculated at 10.2 μm. The boundaries between air and the metamaterial and the metamaterial and InP are at –10 and 10 μm respectively. Purple shows the 1st order mode, blue shows the 5th order mode, and red shows the 9th order mode.

In the second set of simulations, the behavior of individual waveguide modes is further investigated using a transfer matrix method (TMM). Figure 3 shows the calculated electric field profile for select modes with λ = 10.2 μm. The m = 1 mode is a leaky right-handed wave: $v > 0$, the real part of n is smaller than the index of the cladding, and the imaginary part of n is large. The exponentially growing field profile is a valid mathematical solution of the Maxwell equations for such a mode in an infinite planar waveguide. The exponential increase of the field originates from the leaky character of the mode, accompanied with its exponential decay along the y-coordinate [17]. This solution, however, is not a true physical solution to the Maxwell equations. The non-normalizable leaky modes cannot be excited in the real finite-sized structure; a spectrum of normalizable open-waveguide modes with real values of k_x will be excited instead [17].

The m = 5 mode is the first mode that has sub-wavelength field variation, characterized by $v < 0$; however, $|n|$ is smaller than the index of the cladding material and thus the mode is also leaky. The first bound mode with $v < 0$ is the m = 9 mode.

Figure 4(a) shows the calculated real and imaginary parts of the index of refraction for the first 10 modes of the waveguide in the left-handed regime. In this regime, the waveguide supports only higher order modes that have sub-wavelength field variations. The higher order modes have smaller decay lengths into the cladding corresponding to their stronger confinement. The confinement can be further increased and the propagation of lower order negative-index modes can be achieved in thinner (possibly subwavelength) waveguide structures.

The index of refraction for the 5th order mode as a function of wavelength is shown in Fig. 4(b). Both negative and positive index confined ($|n| > 3.1$) propagation is clearly seen for $\lambda >$ 10.7 μm. In the right-handed regime, $\lambda >$ 11.5 μm, the waveguide essentially does not have a cut-off and may support a number of low-index modes in addition to their high-index

#100752 - $15.00 USD Received 29 Aug 2008; revised 25 Sep 2008; accepted 25 Sep 2008; published 29 Sep 2008

counterparts. Here, the limits on mode propagation are governed by the relatively high-index cladding and from deviations of the metamaterial response from the effective medium theory predictions [15]; the system supports a number of strongly confined waves with field variation on the sub-diffractional scale, $\chi^{(e)2} > k^2$.

Highly confined propagation of waves in planar waveguides is accompanied by a dramatic reduction of the modal wavelength $\lambda_o/|n|$ that determines the diffraction limit of planar-waveguide optics [8, 18]. Thus, semiconductor metamaterials open the road for truly nanoscale photonics that combines the benefits of integration with existing semiconductor technology and tunability of the magnitude and sign of the refractive index by modulation of doping level or waveguide size. Anisotropic waveguides can be also used for ultra-compact polarization-control structures and for polarization-sensitive routing of individual modes inside planar systems.

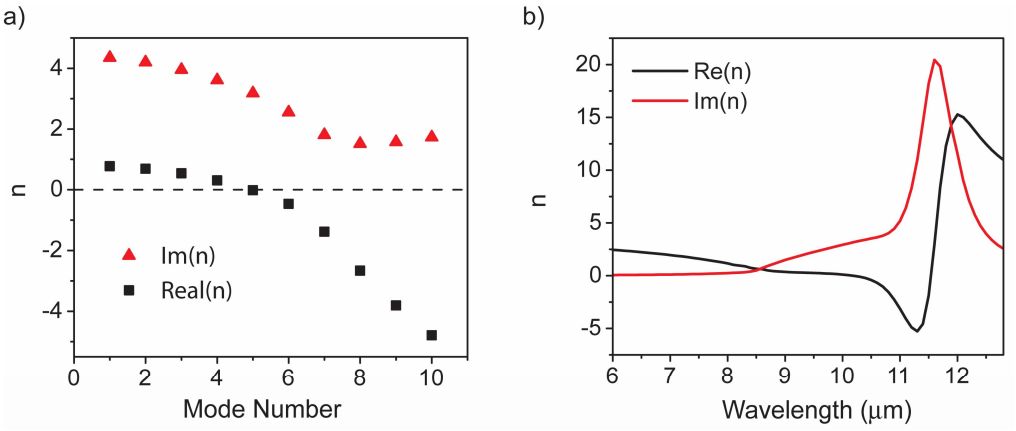

Fig. 4. (a). Real and imaginary parts of n for the first 10 modes at λ = 10.2 μm. (b). Real and imaginary parts of n versus wavelength for the 5th order mode.

4. Conclusion

In conclusion, we have designed and characterized an InGaAs/AlInAs superlattice that behaves as a strongly anisotropic, mid-infrared waveguide. Reflection measurements reveal a low order mode cutoff at λ = 8.4 μm that is characteristic of a sudden sign change in the anisotropy of the metamaterial waveguide and is accompanied by the onset of negative-index propagation of higher order modes. At λ = 11.5 μm the TM reflectivity drops, while TE reflectivity increases, signifying the onset of no-cutoff waveguide propagation. The behavior of the reflectivity and properties of the waveguide modes is confirmed using FE and TMM calculations. Results of numerical solutions are in very good agreement with experimental results. This work was supported in part by PCCM (NSF-ERC), NSF (grant #ECCS-0724763), ONR (grant #N00014-07-1-0457), and ARO. We also acknowledge valuable contributions by E. E. Narimanov and L. Alekseyev in the early phases of this work.

#100752 - $15.00 USD Received 29 Aug 2008; revised 25 Sep 2008; accepted 25 Sep 2008; published 29 Sep 2008